In-plane mixed-mode brittle fracture assessment of Harsin marble using HCSP specimen

Z. Moqadaszadeh, H. Salavati
Shahid Bahonar University of Kerman, Iran
moqadaszadeh@eng.uk.ac.ir, hadi_salavati@uk.ac.ir

M. Rashidi Moghaddam
Shahid Bahonar University of Kerman, Iran, Innovation Center, Barez Industrial Group (BIG), Iran
moghaddam.uni0@gmail.com

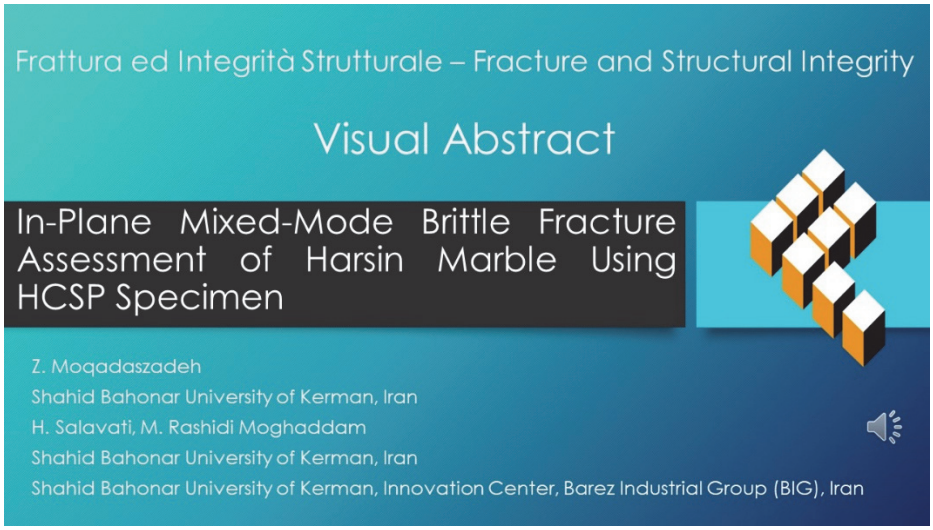

Citation: Moqadaszadeh, Z., Salavati, H., Rashidi Moghaddam, M In-Plane Mixed-Mode Brittle Fracture Assessment of Harsin Marble Using HCSP Specimen, Frattura ed Integrità Strutturale, 68 (2024) 186-196.

Received: 17.11.2023
Accepted: 31.01.2024
Published: 04.02.2024
Issue: 01.04.2024

KEYWORDS. In-plane Mixed-mode, Brittle fracture, Strain energy, T-stress, HCSP specimen.

INTRODUCTION

The three primary fracture modes are referred to as: opening mode (mode I), sliding mode (mode II) and tearing mode (mode III). Engineering components, including cracks, are often subjected to a combination of loading modes due to complex loading conditions. Fracture toughness of quasi-brittle and brittle materials such as ceramics, stones and polymers is an important and necessary material property, because of existing cracks and flaws. Several fracture criteria have been proposed which are classified into three different types like stress-, strain- and energy-based. Erdogan and Sih [1] have been suggested the Maximum tangential stress (MTS) criterion as a stress-based criterion that is utilized widely by researchers on different materials and specimens. SED criterion is an energy-based criterion suggested by Sih [2]. The main concept of this criterion is to measure strain energy density factor (S) in a critical radius (r_c) near the tip of crack. According to the aforementioned criterion, crack propagation happens along an angle θ_0 when S close to the tip of crack attains the critical value (S_{cr}) as being a material property.

According to research works [3,4,13,5–12], conventional criteria like SED and MTS criteria using Williams expansion's singular terms (K_I and K_{II}) could not predict fracture parameters analogous to experimental results achieved from specimens which have a common large characteristic, namely T.

T is the first non-singular high-order term in Williams's series expansion that depends on the geometry and loading configurations. Its value may differ in a wide range for various laboratory test samples. But this effective parameter is constant in line with the crack direction. Fracture parameters of in-plane mixed-mode, especially dominant mode II [6] are variable relative to the significant magnitude and sign of T in a cracked body.

So, researchers offered modified criteria by taking into account the influence of T, like GSED criterion. Ayatollahi et al. [5] developed SED criterion according to the crack parameters K_I, K_{II}, T and revealed the generalized criterion to predict fracture parameters more accurately and give noticeably better values regarding the beginning of fracture in mixed-mode than the SED criterion. Energy-based criteria were not utilized as widely as stress-based criteria to assess the effect of the T on various specimens and materials. So, fracture test using generalized energy-based criteria is required for the purpose of making them sufficiently reliable.

For the purpose of determining the mixed-mode fracture toughness of rocks, various specimens were suggested by researchers. Brazilian disc (BD) [14–18] and semi-circular bending (SCB) [19–22] are two of the widespread and applicable specimens, especially convenient for in-plane mixed-mode loading fracture experiments. Manufacturing each of the specimens begins through drilling an ore to obtain a rock core. After drilling the rock core, circle discs will be made by an electric saw. The procedure always remains the wasted material. Li and colleagues [23] suggested a specimen namely holed-cracked square plate (HCSP) based on the use of the wasted material of BD and SCB manufacturing processes. HCSP specimen has a large T and by changing crack orientation angle (β), pure mode I and II in addition to various combinations of in-plane mixed mode will be simulated. Recently, Li and colleagues [24] utilized HCSP specimen made by PMMA to predict CPA and fracture toughness when exposed to in-plane mixed-mode. Experimental and theoretical results evaluated using a generalized MTS criterion, were then compared.

The objective of this document is studying the effect of T by using HCSP specimen fracture test made of white Harsin marble which has large r_c in compare to PMMA and Also, estimating fracture toughness and CPA using an energy-based criterion namely the GSED criterion.

GSED THEORY

According to the infinite series expansion based on an airy stress function suggested by Williams [25], the elastic stress field near the tip of crack is shown below:

$$\sigma_{rr} = \frac{1}{(2\pi r)^{\frac{1}{2}}}\cos\frac{\theta}{2}\left[K_I\left(1+\sin^2\frac{\theta}{2}\right)+K_{II}\left(\frac{3}{2}\cos\theta-2\tan\frac{\theta}{2}\right)\right]+T\cos^2\theta+O(r^{\frac{1}{2}})$$

$$\sigma_{\theta\theta} = \frac{1}{(2\pi r)^{\frac{1}{2}}}\cos\frac{\theta}{2}\left[K_I\cos^2\frac{\theta}{2}-\frac{3}{2}K_{II}\sin\theta\right]+T\sin^2\theta+O(r^{\frac{1}{2}}) \quad (1)$$

$$\sigma_{r\theta} = \frac{1}{2(2\pi r)^{\frac{1}{2}}}\cos\frac{\theta}{2}\left[K_I\sin\theta+K_{II}(3\cos\theta-1)\right]-T\sin\theta\cos\theta+O(r^{\frac{1}{2}})$$

Consisting of $\sigma_{rr}, \sigma_{\theta\theta}$ and $\sigma_{r\theta}$ as elastic stress components in the polar coordinate system and (r,θ) are conventional coordinates of the crack tip (see fig.1). K_I and K_{II} as singular terms, are the mode I and II SIFs, which are reliant on the conditions of loading and geometric characteristics of laboratory sample. T as a non-singular term, influences on crack growth direction (CGD) and fracture toughness. The higher-order terms $O(r^{\frac{1}{2}})$ close to the crack tip are negligible.

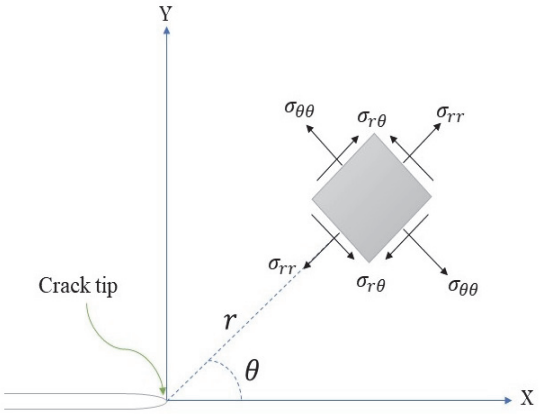

Figure 1: Crack tip stress components in polar coordinates

GSED criterion considers the effect of r_c and T besides singular terms derived from preceding series expansion. The strain energy density function (dW / dV) supplied within an element related to the plane problems is defined as:

$$\frac{dW}{dV} = \frac{1}{2G}\left[\frac{K+1}{8}(\sigma_{rr} + \sigma_{\theta\theta})^2 - \sigma_{rr}\sigma_{\theta\theta} + \sigma_{r\theta}^2\right] \tag{2}$$

where $G(=\frac{E}{2(1+\upsilon)})$ is the rigidity modulus of elasticity and K is an elastic invariable which takes the value of $3-4\upsilon$ and $\frac{3-\upsilon}{1+\upsilon}$ associated to the plane strain and stress problems, respectively. The strength in elastic energy field close to tip of crack is called strain energy density factor (S), and it can be explained as:

$$S = r\frac{dW}{dV} = \frac{r}{2G}\left[\frac{K+1}{8}(\sigma_{rr} + \sigma_{\theta\theta})^2 - \sigma_{rr}\sigma_{\theta\theta} + \sigma_{r\theta}^2\right] \tag{3}$$

By replacing polar stress field components in elastic region from Eqn. (1) into Eqn. (2) and streamlining the aforementioned Eqn. (3), S is outlined below:

$$S = \frac{1}{16\pi G}\left[a_1K_I^2 + a_2K_{II}^2 + 2a_3K_IK_{II} + a_4(\sqrt{2\pi r})K_IT + a_5(\sqrt{2\pi r})K_{II}T + a_6(2\pi r)T^2\right] \tag{4}$$

where $a_i = (i = 1:6)$ coefficients are shown below:

$$\begin{aligned}
a_1 &= (k - \cos\theta)(1 + \cos\theta)\\
a_2 &= [k(1 - \cos\theta) + \cos\theta(1 + 3\cos\theta)]\\
a_3 &= \sin\theta(2\cos\theta - (k-1))\\
a_4 &= \cos\frac{\theta}{2}(\cos(2\theta) - \cos\theta + (k-1))\\
a_5 &= -\sin\frac{\theta}{2}(\cos(2\theta) + \cos\theta + (k-1))\\
a_6 &= \frac{(k+1)}{2}
\end{aligned} \tag{5}$$

Depending on the GSED criterion, crack expansion happens in the angle of direction (θ_0) while the value of S at the r_c from the crack tip is minimum and brittle fracture happens when S attains its critical value (S_{cr}) at a critical radius from the crack tip. Critical value of S and r_c are constant material properties. Angle of crack growth and beginning of fracture is obtained from Eqn. (6) and Eqn. (7) respectively.

$$\begin{aligned} &\frac{\partial S}{\partial \theta}\Big|_{\theta=\theta_0} = 0 \\ &\Rightarrow\ b_1 K_I^2 + b_2 K_{II}^2 + b_3 K_I K_{II} + b_4 (T\sqrt{2\pi r_c}) K_I + b_5 (T\sqrt{2\pi r_c}) K_{II} = 0 \end{aligned} \tag{6}$$

$$\begin{aligned} S_{cr} &= \frac{1}{16\pi G}[a_1 K_I^2 + a_2 K_{II}^2 + 2a_3 K_I K_{II} + a_4(\sqrt{2\pi r}) K_I T + a_5(\sqrt{2\pi r}) K_{II} T + a_6 (2\pi r) T^2] \\ S_{cr} &= \frac{1}{8\pi G}(k-1) K_{Ic}^2 \end{aligned} \tag{7}$$

where $b_i (i = 1:6)$ coefficients are as follows:

$$\begin{aligned} b_1 &= \sin\theta_0 (2\cos\theta_0 - k + 1) \\ b_2 &= -\sin\theta_0 (6\cos\theta_0 - k + 1) \\ b_3 &= (2\cos(2\theta_0) - (k-1)\cos\theta_0) \\ b_4 &= -\sin\frac{\theta_0}{2}(5(\cos(2\theta_0) + \cos\theta_0) + (k+1)) \\ b_5 &= -\cos\frac{\theta_0}{2}(5(\cos(2\theta_0) - \cos\theta_0) + (k+3)) \\ b_6 &= 0 \end{aligned} \tag{8}$$

More details about the GSED criterion are provided in [5]. The SED criterion is obtained by vanishing the terms including the T in Eqn. (6) and Eqn. (7), that these equations are simplified to:

$$\frac{\partial S}{\partial \theta}\Big|_{\theta=\theta_0} = 0 \ \Rightarrow\ b_1 K_I^2 + b_2 K_{II}^2 + b_3 K_I K_{II} = 0 \tag{9}$$

$$S_{cr} = \frac{1}{16\pi G}[a_1 K_I^2 + a_2 K_{II}^2 + 2a_3 K_I K_{II}] \tag{10}$$

HCSP Specimen

Fig. (2) demonstrates loading setup and the geometric characteristics of the HCSP laboratory sample. HCSP refers to a square plate with specific dimensions: it has an edge length denoted as W, a thickness indicated as B, a circular hole in the middle with a diameter of D, and two cracks with a length of 2a, located around the inner hole, radially. Fracture tests are conducted by applying tensile loads (P) which do not need sophisticated loading apparatus put to use in the conventional tensile testing equipment due to the simple geometry of HCSP specimen. HCSP experiences pure mode I loading when the angle of crack orientation in relation to Exerted load (P) is 90°. Each proportion of in-plane mixed-mode will be produced at every angle relative to the applied load. Also, pure mode II loading will be attained at a significant angle which relies on the two other parameters as $2a/W$ and D/W.

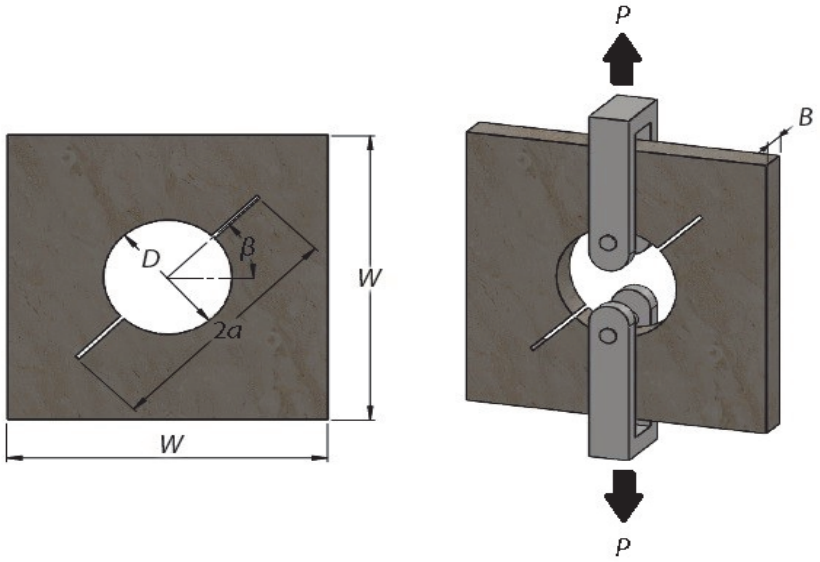

Figure 2: Display of the geometric characteristics and loading setup of a HCSP specimen.

Within the HCSP specimen, the SIFs for both mode I and II, (K_I and K_{II}), along with the T as a non-singular term rely on crack angle inclination (β), ratio crack length to edge length $(2a/W)$ and ratio diameter of circle to edge length (D/W). The SIFs and T within the HCSP specimen stated as [23]:

$$K_i = \frac{P}{B(W-D)}\sqrt{\pi a}Y_i \qquad i = I, II \tag{11}$$

$$T = \frac{P}{B(W-D)}T^* \tag{12}$$

Y_I and Y_{II} represent the geometric factors associated with mode I and II respectively and T^* is the normalized representation of T. Li and colleagues [23] calculated the geometric factors and T^* for multiple values of crack inclination angle (β) within the HCSP by employing the finite element method. The process begins by computing the SIFs and T through simulation of in-plane mixed-mode fracture exposed to a tensile load of arbitrary magnitude. The stress and strain fields are calculated by using the contour integral method of Abaqus software. The mean fracture parameters are then calculated from the values of the middle three of the five concentric contours surrounding the crack tip, as there was no discernible domain-dependence in the brittle model. The dimensionless parameters with regard to sample geometry dimensions were then obtained by substituting the estimated SIFs and T into the Eqn. (11) and Eqn. (12).

The values of Y_I, Y_{II} and T^* for multiple angles of crack orientation (β) are shown in fig. (3). By considering ratios $D/W = 0.4$ and $2a/W = 0.8$ in the HCSP specimen, mode II geometry factor (Y_{II}) is zero for pure mode I $(\beta_I = 0)$ and by increasing crack orientation angle (β) from 0^o to 68^o, Y_{II} increases and mode I geometry factors (Y_I) reduces which are shown in fig. (3). The crack orientation angle in pure mode II loading (β_{II}) equals to 68^o for the HCSP specimen with $D/W = 0.4$ and $2a/W = 0.8$ Variations of T^* from pure mode I to II loading are demonstrated in fig. (3). The value of T^* is negative in the vicinity of pure mode I and II loading and T^* has a large negative value in pure mode II loading. The HCSP has the capability to introduce complete sets of both mode I and II combinations.

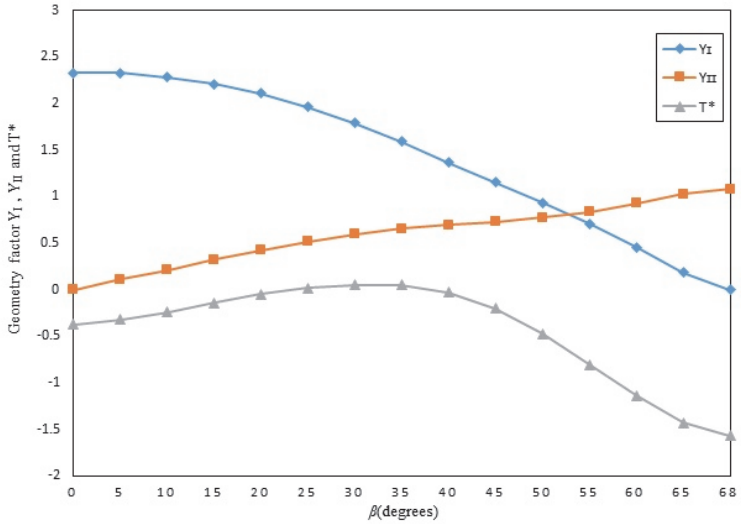

Figure 3: In-plane T* and geometry factors for the HCSP specimen (with D/W=0.4 and 2a/W=0.8).

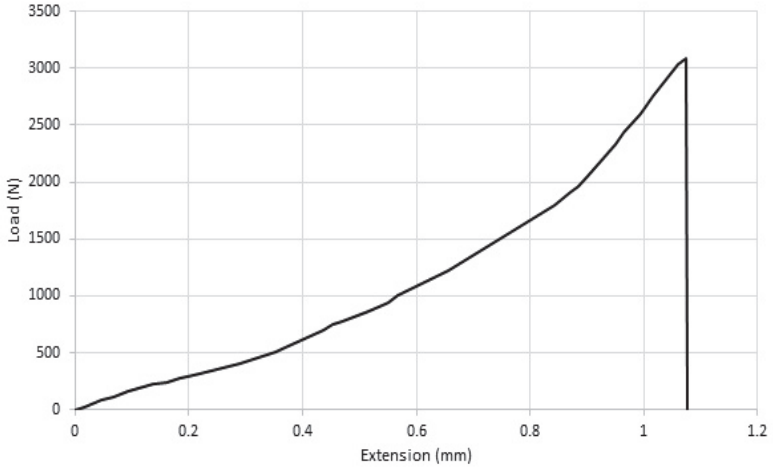

Figure 4: Load-extension curve for HCSP made of white Harsin marble under pure mode II.

FRACTURE EXPERIMENTS

White Harsin marble is one of the homogeneous, uniform, simple cutting and practical rock materials which is available in widespread. Production of HCSP specimen is as follows: at first, a rock cylinder of radius 30 mm from a white Harsin marble block of edge length 150 mm is extracted. Then marble block with a cylindrical hole is sliced into some square plate of thickness 17 mm. An accurate 2D CNC water jet cutting equipment was employed to produce the laboratory samples. Quite slim strip saw blades with a thickness of 0.5 millimeters were utilized to generate artificial radial cracks on the internal hole along the required inclination angles.

Ratios $2a/W=0.8$ and $D/W=0.4$ were considered and angle of crack inclination in pure mode II loading (β_{II}) as indicated in the report of Li and colleagues [23] is $\beta_{II}=68^{o}$. Angles of crack inclination were set to $\beta=\{0$ (pure mode I), 20, 40, 50, 60, 68 (pure mode II)$\}$ degree relating to the HCSP specimen to investigate brittle fracture for covering the entire spectrum of combinations spanning from pure mode I to II. Three samples regarding each angle of crack orientation (β) were manufactured to measure fracture loads. These test specimens were placed within a simple apparatus to apply tensile load on HCSP specimens at an unvarying rate of 0.5 mm/min by a Santam universal hydraulic testing equipment. The load-extension curves were documented while constant monotonic loading. HCSP specimens were fractured from the tip of preset cracks. One of the load-extension curves (pure mode II) for the HCSP

specimen is shown in fig. (4). Relation of load-extension curve shows a linear behavior in fracture test which confirms the linear elastic fracture mechanics (LEFM) hypothesis using for white Harsin marble as a brittle material.
Loads of fracture corresponding to the experimental tests for the HCSP specimens and critical mode I and II SIFs are reported in Tab. (1). By considering the dimensions of the tested samples, the fracture loads and also by extraction of geometric factors (Y_I, Y_{II}) from fig. (3), K_{If} and K_{IIf} are calculated by using the Eqn. (11). Loading setup and crack growth in fractured HCSP specimen are shown in fig. (5).

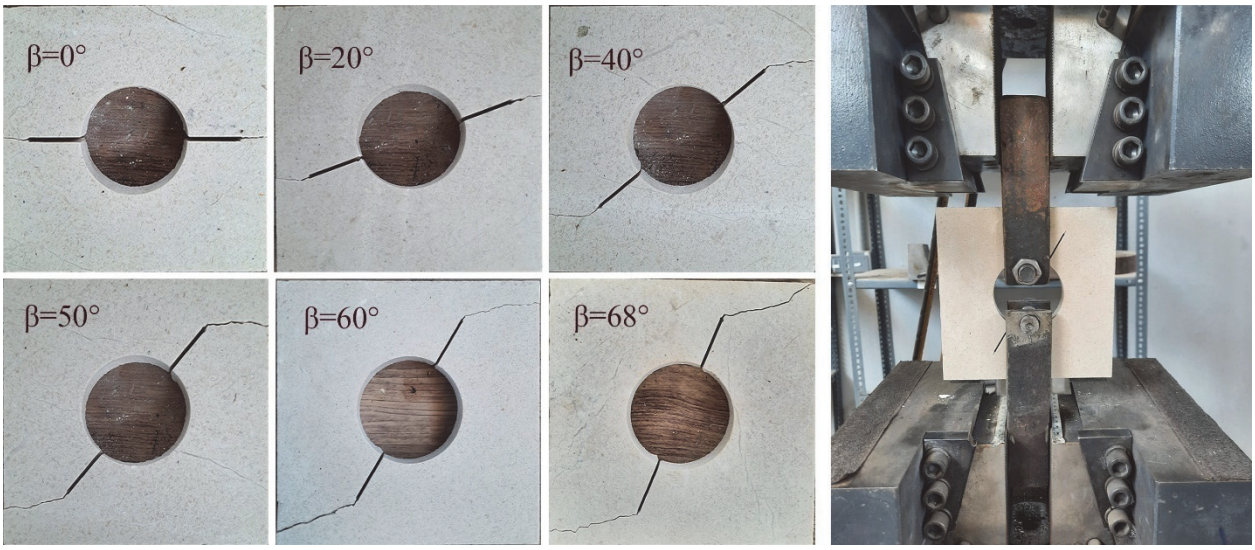

Figure 5: The arrangement for loading and specimens of fractured HCSP with various angles of crack orientation.

Angle (°)	Specimen no.	P(N)	K_{If} ($MPa\sqrt{m}$)	K_{IIf} ($MPa\sqrt{m}$)
0	1	1028	0.48125	0
	2	1028	0.48125	0
	3	1050	0.49125	0
20	1	1071	0.4526	0.0912
	2	1022	0.4321	0.0871
	3	1112	0.4701	0.0948
40	1	1443	0.3956	0.2007
	2	1501	0.4112	0.2087
	3	1485	0.4068	0.2064
50	1	1987	0.3725	0.3075
	2	1875	0.3516	0.2902
	3	1760	0.3301	0.2724
60	1	3213	0.2941	0.5982
	2	3115	0.2851	0.5799
	3	2734	0.2502	0.5089
68	1	3188	0	0.6912
	2	3560	0	0.7721
	3	3101	0	0.6725

Table 1: Loads of fracture and calculated critical SIFs for HCSP specimens.

DISCUSSION

According to the GSED criterion, dimensionless parameters such as Y_I, Y_{II}, T^* and r_c should be specified for calculating beginning and direction of crack propagation. By determining unknown parameters, Eqn. (6) and Eqn. (7) are utilized to predict CPA and fracture toughness. Y_I, Y_{II} and T^* are extracted out of fig. (3) from pure mode I to II loading.

Existing substantial strains or a high quantity of microcracks close to the tip of crack, generate a small destructed region in which the material is strongly damaged and eventually brittle fracture will happen in critical radius starting from the tip of crack. The r_c is the radius of destructed region for rock materials and is not dependent on loading conditions and geometry of specimen. Following the maximum principle stress theory, Schmidt [26] recommended a model for evaluating the size of r_c theoretically:

$$r_c = \frac{1}{2\pi}\left(\frac{K_{Ic}}{\sigma_t}\right)^2 \tag{13}$$

in which K_{Ic} represents the mode I fracture toughness of material which is calculated by using a SCB specimen, experiencing a compressive load according to [27]. Also σ_t is the tensile strength of material which is assessed by using an uncracked BD, subjected to a diametrical compressive load based on [28]. By taking into account the value of $K_{Ic} = 1\ (\text{MPa}\sqrt{\text{m}})$ and $\sigma_t = 7.2\ (\text{MPa})$ of Harsin marble based on [29], the critical radius was calculated from Eqn. (14) as $r_c = 3$ mm .

HCSP specimen is one of the proposed geometries characterized by a substantial negative T in mode II dominant angles. The amount of fracture toughness for the HCSP specimen is dependent on sign and value of T as noted before. Based on the fig. (3), the value of T changes from a low negative (-0.3654) to large negative value (-1.5624) by alteration of the β .

The CPA of fractured HCSP specimens is studied by using of GSED criterion. fig. (7) shows the results predicted from GSED and conventional SED criteria, besides measured CPA results versus a mode mixity parameter which is defined as, $M_e = \frac{2}{\pi}\tan^{-1}\left(\frac{K_I}{K_{II}}\right)$. The value of M_e changes between 0 to 1, in which $M_e = 0$ shows the pure mode II loading and $M_e = 1$ shows the pure mode I loading. A photo was taken from each fractured specimen and from the tip of crack through the crack growth path a line was tangentially drawn to estimate the θ_0 (see fig. (6)). The desired angle was determined by assessing the angle among the tangent line of the CGD and the original crack.

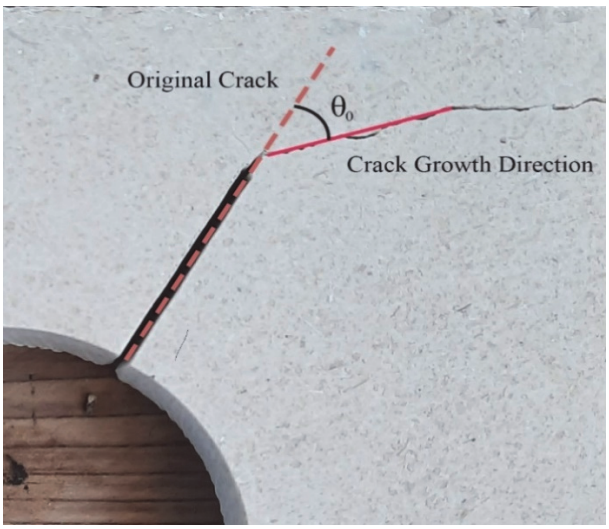

Figure 6: Measurement of the CPA.

Crack growth takes place in a perfectly straight path parallel to the line of original crack when the HCSP is exposed to pure mode I loading. Mixed-mode fracture of HCSP specimens propagates along curvilinear trajectories and does not follow the original crack's line.

It becomes apparent from fig. (7), the angles of crack propagation predicted utilizing GSED criterion are highly consistent with the observed fracture angle of broken HCSP specimens. Negative T decreases the value of predicted CPA in contrary to a positive one. The T led to discrepancy between experimental results and conventional SED criterion especially in mode II dominant angles.

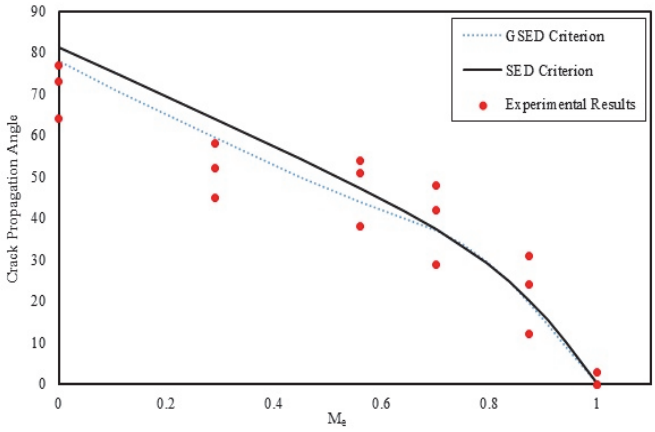

Figure 7: Prediction of GSED criterion for mixed-mode CPA of Harsin marble obtained by HCSP specimen.

New experimental records and theoretical results of in-plane mixed-mode fracture toughness estimation using GSED and SED criteria are shown in fig. (8). The singular terms of the preceding stress field were employed by SED criterion to evaluate the beginning of fracture for a complete spectrum of in-plane mixed-mode loading. Significant discrepancies among experimental and theoretical results provided from conventional SED criterion are shown, especially in mode II dominant angles due to the absence of T (see fig. (8)). The deviation between theoretical predications from SED criterion with experimental results is eliminated by utilizing a generalized criterion which is considering the influence of nonsingular term. According to this generalized criterion, the value and sign of T led to the reduction or increase of in-plane mixed-mode fracture toughness. Although a negative T, enhances the in-plane mixed-mode fracture toughness, the strain energy density capacity is reduced while the T is positive.

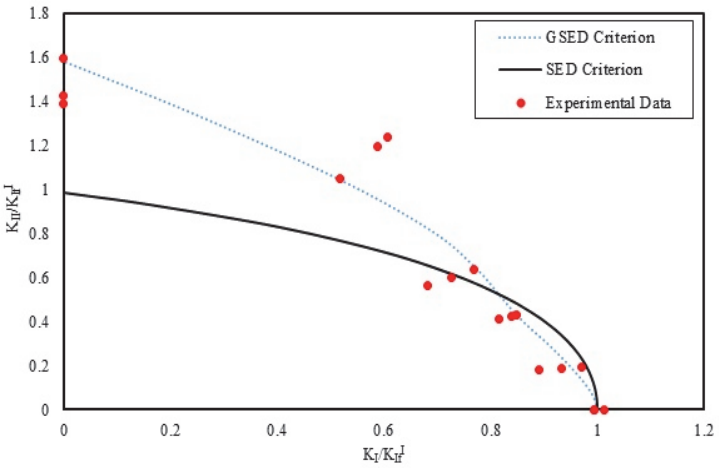

Figure 8: Estimation of GSED criterion for in-plane mixed-mode fracture toughness of white Harsin marble attained by HCSP specimen.

The effect of T is more pronounced for materials having larger value of r_c. According to the fig. (3), the normalized representation of T has a significant value in dominant mode II besides the K_{II} which means the brittle fracture is governed under the influence of singular and non-singular terms. Critical radius of Harsin marble ($r_c = 3\ mm$), Nayriz marble

($r_c = 2.74\ mm$)[30] and Guiting limestone ($r_c = 2.56\ mm$)[31], are a great value in comparison with other brittle and quasi-brittle materials like PMMA ($0.05\ mm \le r_c \le 0.2\ mm$)[24] and PUR foams ($0.388\ mm \le r_c \le 0.596\ mm$)[3]. Hence, Large amount of r_c affects the contribution of T in specimens which are fabricated from rocks.

GSED and SED criteria will predict the same fracture parameters when the magnitude of critical radius is small. Large r_c declares the inconsistency among the values of the experimental records and SED criterion, considerably. The GSED criterion could predict more reliable fracture parameters in comparison with the SED criterion due to consider the influence of r_c and T.

CONCLUSIONS

- ✓ Cheap and convenient HCSP specimen manufacturing and the capability to produce an entire range of in-plane mixed-mode, make the HCSP specimen a suitable candidate to conduct in-plane mixed-mode loading tests of fracture.
- ✓ Large value of T and large r_c of some materials like rocks led to the inconsistency among the reported experimental records and the results predicted theoretically using the SED criterion. Experimental fracture toughness and CPA exposed to mixed-mode loading are in acceptable consistency with the GSED criterion considering the influence of T and r_c besides singular terms (K_I and K_{II}).

REFERENCES

[1] Erdogan, F., Sih, G.C. (1963). Closure to Discussion of 'On the Crack Extension in Plates Under Plane Loading and Transverse Shear', J. Basic Eng., 85(4), pp. 527–527, DOI: 10.1115/1.3656899.

[2] Sih, G.C. (1974). Strain-energy-density factor applied to mixed mode crack problems, Int. J. Fract., 10(3), pp. 305–321, DOI: 10.1007/BF00035493.

[3] Marsavina, L., Berto, F., Negru, R., Serban, D.A., Linul, E. (2017). An engineering approach to predict mixed mode fracture of PUR foams based on ASED and micromechanical modelling, Theor. Appl. Fract. Mech., 91, pp. 148–154, DOI: 10.1016/j.tafmec.2017.06.008.

[4] Ayatollahi, M.R., Rashidi Moghaddam, M., Razavi, N., Berto, F. (2016). Geometry effects on fracture trajectory of PMMA samples under pure mode-I loading, Eng. Fract. Mech., 163, pp. 449–461, DOI: 10.1016/j.engfracmech.2016.05.014.

[5] Ayatollahi, M.R., Rashidi Moghaddam, M., Berto, F. (2015). A generalized strain energy density criterion for mixed mode fracture analysis in brittle and quasi-brittle materials, Theor. Appl. Fract. Mech., 79, pp. 70–76, DOI: 10.1016/j.tafmec.2015.09.004.

[6] Smith, D.J., Ayatollahi, M.R., Pavier, M.J. (2001). The role of T-stress in brittle fracture for linear elastic materials under mixed-mode loading, Fatigue Fract. Eng. Mater. Struct., 24(2), pp. 137–150, DOI: 10.1046/j.1460-2695.2001.00377.x.

[7] Aliha, M.R.M., Ayatollahi, M.R. (2011).Mixed mode I/II brittle fracture evaluation of marble using SCB specimen. Procedia Engineering, 10, pp. 311–8.

[8] Saghafi, H., Ayatollahi, M.R., Sistaninia, M. (2010). A modified MTS criterion (MMTS) for mixed-mode fracture toughness assessment of brittle materials, Mater. Sci. Eng. A, 527(21–22), pp. 5624–5630, DOI: 10.1016/j.msea.2010.05.014.

[9] Ayatollahi, M.R., Aliha, M.R.M. (2007). Fracture toughness study for a brittle rock subjected to mixed mode I/II loading, Int. J. Rock Mech. Min. Sci., 44(4), pp. 617–624, DOI: 10.1016/j.ijrmms.2006.10.001.

[10] Rashidi Moghaddam, M., Ayatollahi, M.R., Berto, F. (2018). Rock Fracture Toughness Under Mode II Loading: A Theoretical Model Based on Local Strain Energy Density, Rock Mech. Rock Eng., 51(1), pp. 243–253, DOI: 10.1007/s00603-017-1319-7.

[11] Ayatollahi, M.R., Aliha, M.R.M. (2008). Mixed mode fracture analysis of polycrystalline graphite - A modified MTS criterion, Carbon N. Y., 46(10), pp. 1302–1308, DOI: 10.1016/j.carbon.2008.05.008.

[12] Aliha, M.R.M., Ayatollahi, M.R. (2009). Brittle fracture evaluation of a fine grain cement mortar in combined tensile-shear deformation, Fatigue Fract. Eng. Mater. Struct., 32(12), pp. 987–994, DOI: 10.1111/j.1460-2695.2009.01402.x.

[13] Negru, R., Marsavina, L., Filipescu, H., Pasca, N. (2013). Investigation of mixed mode I/II brittle fracture using ASCB specimen, Int. J. Fract., 181(1), pp. 155–161, DOI: 10.1007/s10704-013-9830-7.

[14] Awaji, H., Sato, S. (1978). Combined mode fracture toughness measurement by the disk test, J. Eng. Mater. Technol. Trans. ASME, 100(2), pp. 175–182, DOI: 10.1115/1.3443468.
[15] Chang, S.H., Lee, C.I., Jeon, S. (2002). Measurement of rock fracture toughness under modes I and II and mixed-mode conditions by using disc-type specimens, Eng. Geol., 66(1–2), pp. 79–97, DOI: 10.1016/S0013-7952(02)00033-9.
[16] Khan, K., Al-Shayea, N.A. (2000). Effect of specimen geometry and testing method on mixed Mode I-II fracture toughness of a limestone rock from Saudi Arabia, Rock Mech. Rock Eng., 33(3), pp. 179–206, DOI: 10.1007/s006030070006.
[17] Aliha, M.R.M., Ashtari, R., Ayatollahi, M.R. (2006).Mode I and mode II fracture toughness testing for a coarse grain marble. Applied Mechanics and Materials, 5–6, pp. 181–188.
[18] Torabf, A.R., Berto, F. (2014). Mixed mode fracture assessment of U-notched graphite Brazilian disk specimens by means of the local energy, Struct. Eng. Mech., 50(6), pp. 723–740, DOI: 10.12989/sem.2014.50.6.723.
[19] Lim, I.L., Johnston, I.W., Choi, S.K., Boland, J.N. (1994). Fracture testing of a soft rock with semi-circular specimens under three-point bending. Part 2-mixed-mode, Int. J. Rock Mech. Min. Sci., 31(3), pp. 199–212, DOI: 10.1016/0148-9062(94)90464-2.
[20] Ayatollahi, M.R., Aliha, M.R.M., Hassani, M.M. (2006). Mixed mode brittle fracture in PMMA - An experimental study using SCB specimens, Mater. Sci. Eng. A, 417(1–2), pp. 348–356, DOI: 10.1016/j.msea.2005.11.002.
[21] Ayatollahi, M.R., Aliha, M.R.M., Saghafi, H. (2011). An improved semi-circular bend specimen for investigating mixed mode brittle fracture, Eng. Fract. Mech., 78(1), pp. 110–123, DOI: 10.1016/j.engfracmech.2010.10.001.
[22] Kuruppu, M.D., Chong, K.P. (2012). Fracture toughness testing of brittle materials using semi-circular bend (SCB) specimen, Eng. Fract. Mech., pp. 133–50, DOI: 10.1016/j.engfracmech.2012.01.013.
[23] Li, Y., Pavier, M.J., Coules, H. (2020).A new specimen for mixed mode I/II fracture of brittle and quasi-brittle materials. Procedia Structural Integrity, 28, pp. 1140–7.
[24] Li, Y., Pavier, M.J., Coules, H. (2021). Mixed-mode brittle fracture test of polymethylmethacrylate with a new specimen, Fatigue Fract. Eng. Mater. Struct., 44(4), pp. 1027–1040, DOI: 10.1111/ffe.13411.
[25] Williams, M.L. (1957). On the Stress Distribution at the Base of a Stationary Crack, J. Appl. Mech., 24(1), pp. 109–114, DOI: 10.1115/1.4011454.
[26] Schmidt, R.A. (1980).A microcrack model and its significance to hydraulic fracturing and fracture toughness testing. 21st U.S. Symposium on Rock Mechanics, USRMS 1980, pp. 581–90.
[27] Fowell, R.J., Hudson, J.A., Xu, C., Chen, J.F., Zhao, X. (1995). Suggested method for determining mode I fracture toughness using Cracked Chevron Notched Brazilian Disc (CCNBD) specimens, Int. J. Rock Mech. Min. Sci., pp. 57–64, DOI: 10.1016/0148-9062(94)00015-U.
[28] Li, D., Wong, L.N.Y. (2013). The brazilian disc test for rock mechanics applications: Review and new insights, Rock Mech. Rock Eng., 46(2), pp. 269–287, DOI: 10.1007/s00603-012-0257-7.
[29] Aliha, M.R.M., Ayatollahi, M.R., Akbardoost, J. (2012). Typical upper bound-lower bound mixed mode fracture resistance envelopes for rock material, Rock Mech. Rock Eng., 45(1), pp. 65–74, DOI: 10.1007/s00603-011-0167-0.
[30] Mirsayar, M.M., Razmi, A., Aliha, M.R.M., Berto, F. (2017). EMTSN criterion for evaluating mixed mode I / II crack propagation in rock materials, Eng. Fract. Mech., DOI: 10.1016/j.engfracmech.2017.12.014.
[31] Moghaddam, M.R., Ayatollahi, M.R., Berto, F. (2017). Mixed Mode Fracture Analysis Using Generalized Averaged Strain Energy Density Criterion for Linear Elastic Materials, Int. J. Solids Struct., DOI: 10.1016/j.ijsolstr.2017.04.035.